Heart Monitor Using Flexible Capacitive ECG Electrodes

Yang Gao, Varun V. Soman, Jack P. Lombardi, Pravakar P. Rajbhandari, Tara P. Dhakal, Dale Wilson, Mark Poliks, Kanad Ghose, James N. Turner, Zhanpeng Jin

***Abstract*—Non-invasive sensors capable of measuring weak bio-potential signals such as ECG and EEG and communicating results wirelessly to a host computer are developing rapidly. Some of them utilize capacitively-coupled electrodes in an attempt to place the sensor at a distance from the skin. This study demonstrated the fabrication and development of a capacitively-coupled ECG electrode prototype using custom high specific capacitance electrodes and custom high performance electronics. Two ultra-thin capacitive electrodes were fabricated on a flexible polyimide substrate (2 by 2 inches) protected by a guard ring to reduce noise. The detection and amplification circuitry consisted of op-amps that filtered and conditioned the ECG signal. R-peaks in the ECG were readily detected and quantified using both simulated signals from ECG databases and real signals from human subjects. Heart rates and heart rate variability calculated from our monitor measurements were comparable with commercial rigid wearable sensors, including a smartwatch and an ECG monitor that uses standard clinical ionic electrodes. The prototype monitor was tested on human subjects during rest and moderate exercise and showed appropriate responses. The challenge of high-gain low-noise amplification was met by the development of highly thinned operational amplifiers whose operation was shown to be equivalent to commercially available rigidly packaged operational amplifiers, demonstrating that high performance Si- electronics can be used to produce high-fidelity signals from weak biopotentials.**

***Index Terms*—ECG, capacitive electrode, health monitoring, heart rate**

I. Introduction

WEARABLE sensors for human activity monitoring have drawn considerable attention in recent years [1], [2], [3], [4], [5], [6]. They could be very useful in providing accurate real-time information of human vital signs, especially for monitoring the electrocardiogram (ECG) signal [7]. Compared with traditional healthcare instrument, wearable ECG sensors provide great convenience for long-term monitoring and portability. But like any other mobile devices, they still have some major constraints, including power consumption and the skin-electrode interface [8], [9], [10]. However, integration of chips and discrete component circuitry, with noise filtering capability, can provide good performance, but this requires consuming more power from the battery. This is a major trade-off as long-term operation is important for wearable health monitors. Most wearable ECG sensors [11], [12], [13], [14] acquire signals by utilizing wet electrodes, which use low-impedance ionic gels, usually Ag/AgCl, to ensure good contact between the monitor's input and the skin. However, gels suffer from electrical instability due to humidity, sweat, drying, and smearing across the skin over time [15]. The gels and adhesives have other drawbacks as well, including skin irritation and disturbance of daily activities [16], [17]. Some patients are sensitive to the gel, which can cause an allergic reaction [18].

To improve mobility and comfort, dry electrodes and capacitive electrodes are being developed [16], [19]. Dry electrodes minimize allergic reactions, reduce preparation time, and can be fabricated from many conductive materials. Generally, there are two kinds of dry electrodes: spike arrays [20] and soft materials [21]. The spikes ensure good electrical and mechanical contact with the skin. In [22], a 3D printed dry electrode with 180 conical needles (distance=250 μm) was proposed. The needle length was larger than nano or micro needles, to allow operation on hairy skin. However, they suffer from high motion artifacts due to the limited contact area. In [23], a novel polymeric dry electrode with a metal layer on a poly-di-methyl-siloxane (PDMS) substrate was described. These electrodes had better skin compatibility and motion artifact tolerance compared with spike electrodes. However, dry electrodes still require an electrically conductive material to be in direct contact to skin, which is not convenient and presents safety concerns. Thus, non-contact or capacitively-coupled electrodes have also been explored. Non-contact means a capacitor is formed by the electrode plate, which is covered with a dielectric, and the skin. The capacitor will convert ECG biopotential signals into an electrical signal by charging and discharging the capacitor. The capacitive electrode is convenient and is relatively easy to implement [24], but at the cost of high electrode impedance and weak signal amplitude. In [25], a coin-sized capacitive electrode was used for a body sensor network. Each electrode senses the local biopotential and a differential voltage can be measured. However, the multiple electrode nodes are hard to fix in place and are prone to motion artifacts.

In this work, we report the development of a prototype ECG human performance monitor (HPM) that incorporates capacitive electrodes and a non-chip front-end circuit. Compared with the traditional wearable ECG, our approach can provide a better skin-contact interface, without sacrificing signal quality and sensor portability. Our contributions can be summarized

Y. Gao and Z. Jin are with the University at Buffalo, State University of New York, Buffalo, NY, 14260, USA, email: {ygao36, zjin}@buffalo.edu. This work was done when Y. Gao and Z. Jin were at the Binghamton University.

V. V. Soman, J. P. Lombardi, P. P. Rajbhandari, T. P. Dhakal, M. Poliks, K. Ghose, and J. N. Turner are with the Binghamton University, State University of New York, Binghamton, NY 13902, USA, email: {vsoman1, jlombar4, prajbha1, tdhakal, mpoliks, ghose, jturner}@binghamton.edu.

D. Wilson is with the American Semiconductor, Inc., Boise, ID, 83709 USA, dalewilson@americansemi.com.

as:

- We achieved a better and flexible skin-contact interface by deployment of a non-ionic capacitive electrode.
- We designed the simplified signal conditioning circuit by only using 4 op-amps instead of employing a highly integrated analog front-end chip.
- We validated the effectiveness of heart rate detection through the monitored ECG signals using the proposed system on human subjects under different scenarios, and compared the performance with measurements recorded using commercially available devices.

The remainder of this paper is organized as follows: Section II introduces state of art of ECG monitoring and different types of electrodes; Section III describes the system structure and the two major prototype subsystems, signal conditioning circuit and capacitive electrode design; the experimental setting and the evaluation of results are discussed in Section IV and V; and Section VI presents our conclusions and recommendations for future research.

II. Monitor Design

To achieve an acceptable trade-off between wear-ability and signal quality, our human performance monitor (HPM) was designed as a flexible hybrid electronic (FHE) device, which means that it has a flexible substrate with rigid islands where conventional Si electronics and a battery are mounted. A one-lead ECG dual electrode system captured the ECG signal, and a peripheral guard ring provided extra noise shielding. High specific capacitance electrodes were developed using a high dielectric nanolaminate that allowed the electrode foot-print to be reduced. Since the detected signals are so low, a very high gain low noise front end amplification circuit was initially developed using high quality commercially available operational amplifiers (OpAmps). The present version is in the form of a prototype with the capacitively-coupled electrodes fabricated on a Ube Plastics UPILEX 125S polyimide substrate hard wired to the development circuitry mounted on a printed circuit board (PCB). Two versions of the circuitry compared the performance of the HPM using commercially available high-gain OpAmps to thinned silicon FleX^{TM} ASOPA4002, OpAmps developed by American Semiconductor Inc., Boise Idaho (AmSemi).

A. Prototype System

As shown in Fig. 1, the ECG monitoring prototype system involves two major subsystems: the flexible capacitive electrodes and a PCB-based chip-on-board design (1.5 inch $\times$ 1.5 inch) powered by a 3-V single Lithium ion cell battery. The Ube Plastics UPILEX 125S polyimide substrate based capacitive electrodes capture the weak bio-electrical signal from the heart's activity and sends it to the PCB. After amplification by the front-end and differential modules, the signals are processed through the noise filtering module composed of band pass and notch filters. A 11-bit ADC converts the analog signal to the analyzable digital ECG signal.

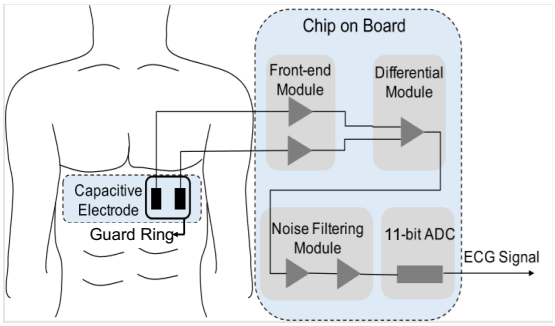

Fig. 1. Block diagram of the ECG monitor.

1) Capacitive Electrodes: Capacitive electrodes have the advantage of either being non-contact electric field detectors or at least having an isolating dielectric layer between the metal electrode and the skin. Capacitive electrodes sense the ECG signals by coupling them capacitively to a voltage follower amplifier instead of using direct body contact. This substantially reduces the possibility of inadvertently injecting current into the body. Unless they are securely attached to the subject, the capacitive electrodes can separate from the body and introduce an airgap that can reduced the coupling capacitance significantly, reducing the sensed signal amplitude. A design goal for capacitive electrodes is thus to avoid the airgaps and use high-K dielectric materials to enhance the specific capacitance (capacitance per unit area) to increase the signal amplitude sensed by the voltage follower amplifier, given realistic area constraints.

A single electrode would provide better wear-ability, but it is more easily affected by electrical noise. In contrast, multiple electrode systems produce higher signal quality but is less wearable. A two-electrode design was chosen as a trade-off between signal quality and wearability. The two electrode design uses closely-placed electrodes with a differential readout that rejects common mode noise.

Fig. 2 represents the typical bipolar ECG sensor placement and their corresponding ECG waveforms. As shown, the information gathered between aVR, aVL and aVF is known as "bipolar" leads, which form an Einthoven's triangle and divide the chest space into three regions. The QRS complex from each region has a different polarity. Optimum mounting of the monitor involved selecting a body site with as large a flat and smooth area as possible, that is flexed and twisted as little as possible. Further, it had to be away from the central chest area to minimize the effect of any currents that might be injected into the body, including those from the most extreme failure modes. Thus, we chose the rib cage below the Lead III region which has positive QRS peak amplitudes, reasonable proximity to the heart but is away from the most critical areas for potential current injection.

Fig. 3 (a) shows two capacitive electrodes of 400 mm^2 and a surrounding guard ring that reduces interference from the skin (e.g., static electric). The electrodes were two 1 μm thick copper rectangles with maximum electrode separation on a 2X2" Ube Plastics UPILEX 125S polyimide substrate. In the cross-sectional view (b), a ceramic nanolaminate dielectric layer was deposited on the electrodes to provide high capac-

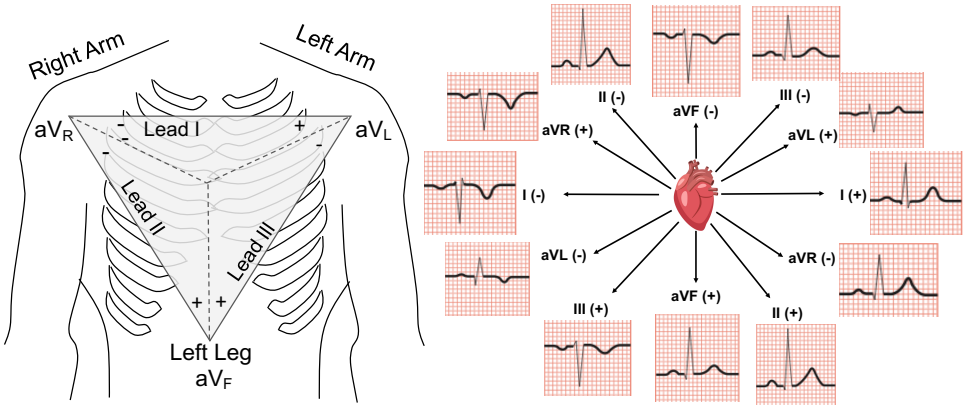

Fig. 2. ECG sensor placement

itance. To reduce the noise caused by body motion artifacts, a conductive foil tape attached on the guard ring was used to fix the electrodes' position on the body. The electrodes were fabricated using an etch back process and additive techniques to allow rapid fabrication and easy modification of the electrode design. CAD layouts of electrodes of 400 mm^2 are shown in Fig. 3. A 100-nm titanium adhesion and 1 μm copper layers were deposited on a 125 μm (5mil) Ube Plastics UPILEX 125S substrate using a KDF inline sputter deposition system. After metal deposition, a photoresist mask was printed on the copper using an Optomec AJ-300 aerosol jet printer with the ultrasonic atomizer loaded with MicroChem S1805 photoresist. The printed masks were baked at 90 °C for 2 min to dry and solidify the photoresist. The copper layer was wet-etched using Transene CE-200 ferric chloride based copper etchant diluted 1:5 with DI water. The samples were etched until clear, approximately one minute. The titanium was dry etched in a Nano Master NRP-4000 PECVD/RIE system with a 5 min fluorine based SiO_2 etch. The patterned electrodes and traces were cleaned with acetone and isopropanol to remove the photoresist and blown dry with nitrogen.

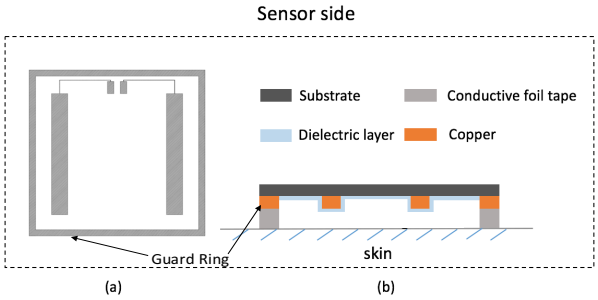

Fig. 3. Capacitive electrode design (a) top view; (b) cross-sectional view

The dielectric layer was deposited using atomic layer deposition (ALD), that previously demonstrated a high value of dielectric constant [26]. The TiO_2 – Al_2O_3 nanolaminate dielectrics were deposited as a stack of 166 alternate layers of Al_2O_3 (3 Angstroms thick) and TiO_2 (3 Angstroms thick) using a Sundew Technologies D200 ALD system (Figure 4). The purpose of stacking the alternate layers is to increase the dielectric constant due to the Maxwell-Wagner relaxation principle [27]. These nanolaminates were sandwiched between Al_2O_3 capping layers on top and bottom of the stack to decrease the leakage current (Fig. 4). This resulted in a dielectric layer with an approximate thickness of 103 nm. The ALD deposition of TiO_2 was performed using Titanium Tetrachloride ($TiCl_4$) and water (H_2O) as precursors and the Al_2O_3 was deposited using trimethylaluminum (TMA) and water (H_2O) as precursors. The deposition of the dielectric layer was carried out at 200 °C. A typical TiO_2 – Al_2O_3 nanolaminate capacitor with 6nm Al_2O_3 capping layers between two metal electrodes of area 0.09 cm^2 showed a capacitance of 0.53 μF/cm^2, a breakdown voltage of 7.5 V, a leakage current around 100 nA, and a dielectric constant of 120 at frequencies up to 100kHz. In actual use, however, the human skin acted as the top layer of the capacitor. Due to the large area of the capacitors and lack of a top metallic layer, it was difficult to measure total capacitance of the operational configuration.

Electrode geometry is very important, not only to provide a large capacitance and better signal quality, but also to provide wear-ability. Thus, to find the best trade-off between electrode size and separation, we tested several geometric configurations with electrode sizes of 50, 100, 400 mm^2 and spacing of 15 and 30 mm as shown in Figure 5 using the same front-end circuit. After comparing the output ECG signals, the larger electrode and wider separation produced the best signal quality recordings (data not shown). Thus, the final design used 400 mm^2 electrodes with 30 mm separation.

2) circuit design: Front-end Module: The capacitance of the electrode (Cs) mainly depends on the electrode area (A), relative static permittivity or dielectric constant (ϵ_r), the electric constant (ϵ_0), and the dielectric thickness (d). In our model with an air gap between the electrode and the skin, Cs ranges from 7 pF to 35 pF.

$$C_s = \epsilon_0 \epsilon_r \frac{A}{d} \tag{1}$$

Due to the extremely small capacitance, an impedance-matched front-end circuit was placed between the electrode and the differential amplification module to avoid degradation of the weak ECG signals, as shown in Fig 6.

3) Bias with resistor: A large resistor was used to provide a bias current to the operational-amplifier [28]. The capacitor (Cs) in series with the bias resistor, R_{bias}, forms a high-pass filter. The cutoff frequency (F_{cut}) is determined by:

$$F_{cut} = \frac{1}{2\pi C_s R_{bias}} \tag{2}$$

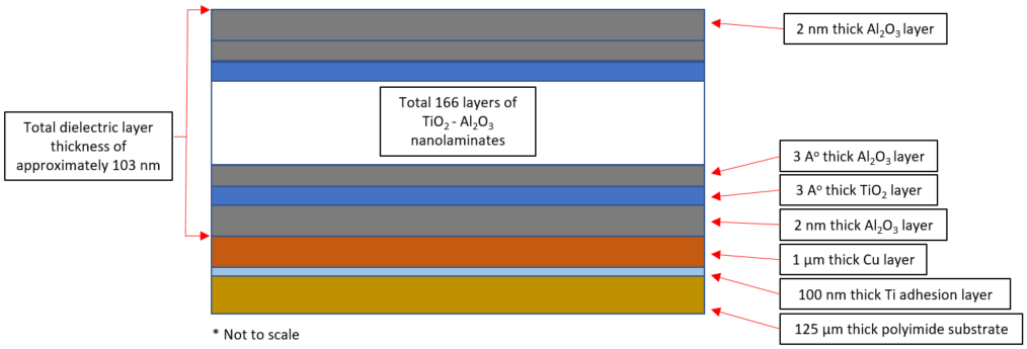

Fig. 4. The cross-sectional view of the capacitively-coupled electrode

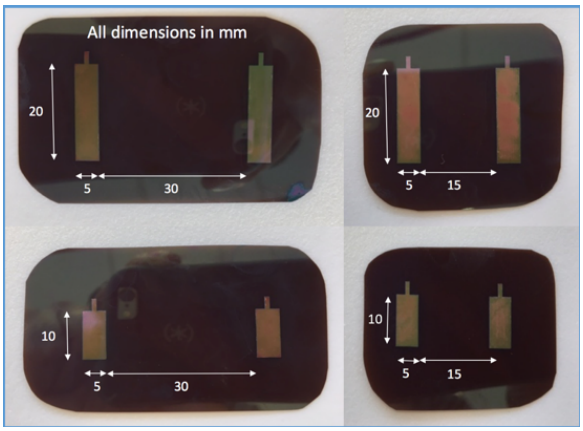

Fig. 5. Four tested electrode geometries

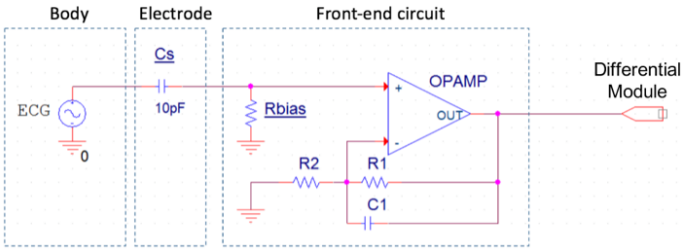

Fig. 6. Front-end equivalent circuit model

To avoid filtering out the information in the ECG spectrum below 10 Hz, R_{bias} should be at least 2 GΩ. To achieve the best trade-off between lower current noise and the ECG waveform spectrum, we used a 5 GΩ resistor, which sets the cutoff frequency at a few Hz. To provide the ECG signal with better stability, we also added a phase-compensate capacitor C_1 in parallel with R1, which behaviors as a low-pass filter in the negative feedback loop.

4) High input-impedance amplifier: To minimize signal degradation, the preamplifier input impedance should be as high as possible. Thus, we tested TI′s LMC6442 operational amplifiers and American Semiconductor, Inc's PSOPA4002 op-amp. Both have a very high input impedance low input offset current, (a few fA), and an operational voltage that can be supplied by the CR2032 coin cell battery.

5) Differential Amplification Module: To remove the noise from the common mode signals, the two signals from separate electrodes are fed into a low-power instrumentation op-amp

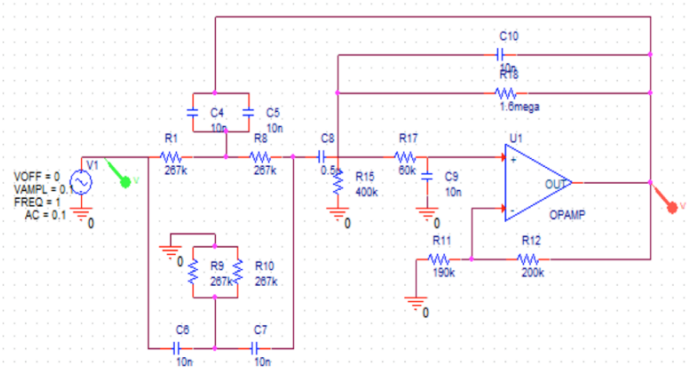

Fig. 7. Circuit schematic of notch and band-pass filter

INA118 with 350 μA quiescent current and 50 μV offset voltage in the differential module. A 1 $k\Omega$ resistor is set to acquire X50 gain, which initially amplifies the output differential signal.

6) Noise Removal: Guard Ring & Filtering Module: ECGs are subject to various noise sources internally (e.g., muscle activity and baseline shift by respiration) and externally (e.g., power-line noise and motion artifacts). These noise sources can be largely filtered out by commercial front-end chips (e.g., AD8232 or ADS1298), however, the high integration on chip also brings high power consumption, which might not be suitable for long-term ECG monitoring. Thus, a passive filter was added in the form of a copper guard ring shielding the electrodes from outside noise, see Fig. 1 and Fig. 3.

As shown in Fig. 7, to reduce the power consumption, instead of using a commercial chip or two cascaded op-amps, we utilized a twin-T notch filter (removal of 60 Hz power-line noise) and a band-pass filter (0.3 to 100 Hz) (Fig. 8) followed by amplification with a single op-amp (Fig. 7). The performance of this filter is shown in Fig. 8. The cutoff frequencies of 0.3 to 100 Hz with a notch at 60 Hz are optimum for ECG signal detection.

III. Flexible High Performance Silicon Electronics

A wearable ECG sensor ideally implements the capacitive electrodes, amplification and processing circuitry and microcontroller all on a single flexible substrate. Towards the realization of this goal, the front-end amplification circuitry

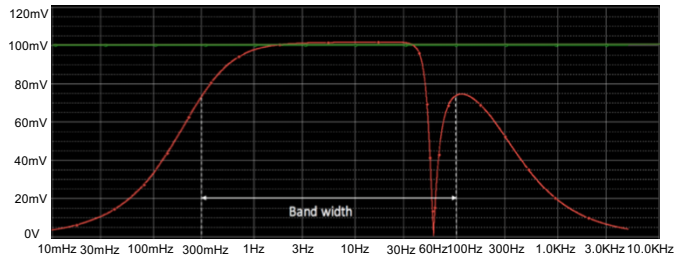

Fig. 8. Frequency response of the filter design in Figure 7. Green line is the input (DC sweep), red line is the output response, the cut-off frequencies are 0.3 Hz and 100 Hz, and there is a notch at 60 Hz for removal of this frequency.

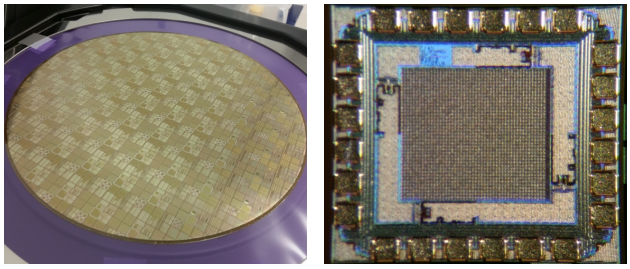

(a) (b)

Fig. 9. FleX Wafer with ASOPA4002 FleX-OpAmps on Dicing Tape (a) and individual FleX-OpAmp Die (b).

TABLE I
FLEX-OPAMP PHYSICAL CHARACTERISTICS

Die Size	2.4 mm X 2.4 mm	Pad Pitch	300 μm
Pin Count	24	Thickness	25 μm
Pad Openings	160 μm X 160 μm	Flexible	Yes
Pad Bumps	10 μm Ni/Au	Conformal	Yes

was implemented using thinned-die opamps on a flexible substrate. A full implementation with all of the electronics and the capacitive electrodes on a single substrate was not possible as a suitable microcontroller was not available as a thinned die. To compare the performance of the front-end circuitry using thinned dies on a flexible substrate, a discrete component realization of the same circuitry was also implemented.

Human subject measurements were used to compare conventional, Texas Instruments′ (TI) op-amp LMC6442, and the custom flexible, American Semiconductor Inc's Boise Idaho (AmSemi) FleX™ ASOPA4002, OpAmps in the Front-end Module's amplification circuitry. The AmSemi OpAmps are highly flexible bare dies of thinned Si designed to be mounted on flexible substrates, while having all the advantages of high-speed Si electronics. Thus, they are ideal for wearable devices, including medical sensors. The TI OpAmps are conventional rigid packaged modules. The concept and motivating factor for flexible hybrid electronics (FHE) is the need to enable printed materials with high-performance electronic capability for digital logic, digital memory, analog circuits and radio frequency (RF) communication. This vision relies on the integration of high performance silicon CMOS integrated circuits (ICs) that are necessary for any sufficiently complex FHE system. Conventional silicon ICs provide the best performance and the most mature technology for high-performance microelectronics. Modern CMOS IC′s are unparalleled in performance and provide advantages in circuit density, power and speed that cannot be replicated with printed components. For example, even mainstream low cost 8-bit microcontrollers, considered relatively simple in the IC industry, operate below 1.5V and can include more than 2 million transistors and provide many orders of magnitude higher performance than the best printed transistor circuits. However, traditional CMOS ICs are rigid making them ill-suited for truly flexible and conformal applications. American Semiconductor′s FleX™ Semiconductor-on-Polymer™ (SoP) process converts standard CMOS devices into an ultra-thin ($< 40\mu m$), fully flexible format. The SoP process removes nearly all the silicon replacing it with a thin layer of polymer to provide mechanical stability without sacrificing flexibility. The SoP ICs retain the full functionality of their conventional CMOS counterparts.

American Semiconductor designed, manufactured and tested a quad operational amplifier IC for integration into the prototype monitor. The FleX-OpAmp (ASOPA4002) was selected as the initial candidate for FleX conversion as it was desired to move the signal amplification as near to the capacitive sensors as possible. Bringing the amplification near the sensors improves the system signal-to-noise ratio and thereby allows detection of lower signal levels and improved signal fidelity.

The FleX-OpAmps were designed in the TowerJazz CS18 0.18 μm SOI CMOS process with four levels of aluminum interconnect. The standard processing of the full thickness wafers was completed by TowerJazz. American Semiconductor then completed the FleX Silicon-on-Polymer wafer process to convert them to the desired ultra-thin, flexible format. Figure 9 (a) is an image of one of the completed FleX wafers mounted to a thermal dicing tape on a dicing frame. Figure 9 (b) is a magnified image of a single FleX-OpAmp die. The FleX-OpAmp physical characteristics are provided in Table I. The bond pad openings and the pitch were intentionally made larger than typical for ICs to facilitate easier assembly into the resulting FHE system.

Each of the four on-board operational amplifiers in the quad op amp IC are low noise and high performance to provide maximum utility in a wide range of flexible system applications. Table II provides some key performance metrics comparing the program design targets with our measured results. Additionally, FleX-ICs have successfully completed a wide range of testing including: static radius of curvature down to 1mm, dynamic radius of curvature, high and low temperature operating life, electrostatic discharge, and scanning electronic microscopy delayering analysis.

As shown in Fig. 10, the two traces are very similar and both produced high-fidelity R-peaks that are easily detected and analyzed, and both traces have essentially the same slowly varying baseline. Thus, the FleX-IC™ OpAmps are clearly a good choice for future developments that need high-gain low-noise signal amplification and flexible conformal components.

IV. PERFORMANCE EVALUATION

The evaluation was divided into three parts: 1) electric testing of the circuit; 2) functional testing with simulated sig-

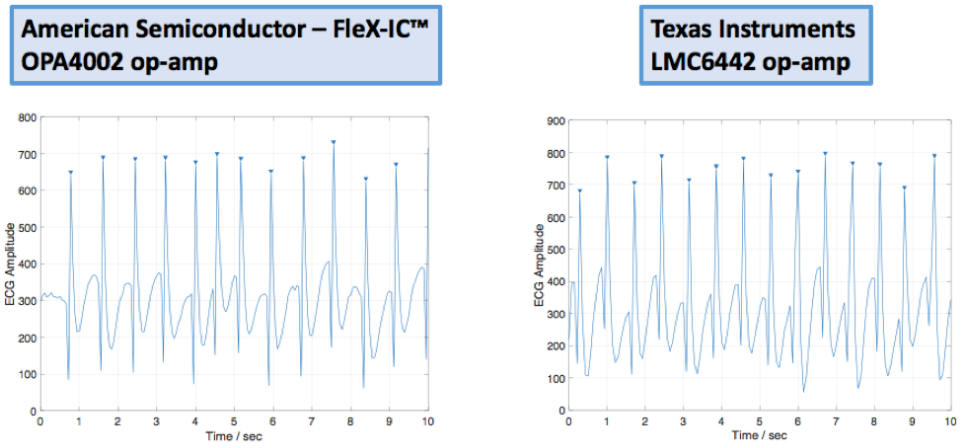

Fig. 10. R-peaks traces from a human subject using the AmSemi flexible OpAmps (left) and the TI conventional hard packaged OpAmp (right).

TABLE II
FLEX-OPAMP KEY PERFORMANCE METRICS - DESIGN TARGET VERSUS MEASUREMENT RESULTS

Parameter	Target	Measured
Supply Voltage	2.25-2.75 V	0.8-2.75 V
Gain-Bandwidth	>200 kHz	5M Hz
Open Loop Gain	>80 dB	>90 dB
Slew Rate - Rise	>0.2 V/ μ s	4.5 V/ μ s
Slew Rate - Fall	>0.2 V/ μ s	4.1 V/ μ s
Output Swing	0.1 - 2.4 V	0.06 - 2.45 V
Input Offset Voltage	<5.0 mV	<100 μV
Input Offset Current	<1 nA	<5 pA
Input Impedance	>1 GΩ	>100 GΩ
Unity Gain Stable	Yes	Yes
Power Dissipation	2 mW	3 mW
ESD Rating (Human Body)	2 kV	4 kV

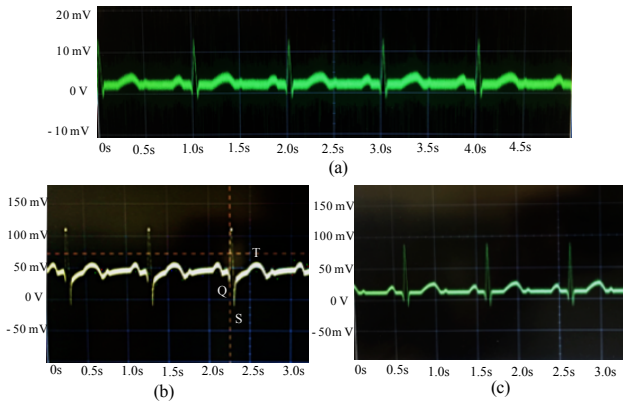

Fig. 11. (a) Archived ECG signal (10 mV); (b) Output from ASOPA4002 (AmSemi); (c) output from LMC6442 (Texas Instrument).

nals from ECG databases (i.e., MIT-BIH Arrhythmia Database [29], [30]), validating the system's response to known certified inputs; and 3) human subject testing. Three human subjects wore capacitive electrodes hardwired to a PCB version of our circuitry. All human subject testing was carried out in compliance with Binghamton University's Internal Review Board Protocol 14-3267. To evaluate the performance of the noise filtration, the circuit was simulated using OrCAD Capture. As shown in Fig. 8, the band-pass cut-off frequency at 0.3 Hz and 100 Hz, which filtered out signal components caused by electromyogram (EMG) and respiration. In addition, a notch filter also filtered out the 60-Hz power-line interference. The functionality of the entire circuit was validated by inputting a synthetic ECG signal. The system's operation was verified for two operational amplifiers in the amplification stage: 1) American Semiconductor's Fle™ Semiconductor-on-Polyme™, and 2) the dual in-line package op-amp LMC6442 from Texas Instruments. The results using a 5 mV archived ECG signal as the input are shown in Fig. 11. Both outputs show a clear ECG waveform with QRS peak and other components (e.g., P and T peaks) verifying the circuit's operation and showing that the two OpAmp amplifier systems are equivalent. Output waveform using op-amp ASOPA4002 has a slight distortion and drift on S peaks between QT intervals. The trailing edge on S peaks might result from its larger input offset current (<5 pA) compared with op-amp LMC6442 (<0.025 pA) especially when the input impedance is large.

To compare our monitor with commercially available units, all human subjects wore a commercial ECG monitor (Shimmer 2) with gel electrodes, a smartwatch with an ECG light-sensor (Huawei Smart Watch), and our ECG monitor with capacitive electrodes. For the Shimmer 2 ECG kit, three limb wet electrodes (RA, LA, LL) and one reference electrode (RL) were placed on the subject's chest. The output ECG signal was sampled at 500 Hz. The Smart Watch was placed on the subject's wrist and the heart rate was measured using the built-in photoplethysmography (PPG) sensors. In Figure 12, we divided the test into three phases: 1) 2-minute rest (i.e., participants sat on a chair with our monitor attached on the lower left part of the chest); 2) 2-minute mild exercise (i.e., participants ran in place at low speed); and 3) 5-minute rest (i.e., participants sat back on a chair).

The capacitive electrodes, as shown in Fig. 1, were worn on the lower left rib cage such that the electrodes were along an axis aligned with the heart. The electrodes were hardwired to the PCB circuitry that was mounted nearby. The detected signals from our prototype monitor and from the Shimmer 2 using standard clinical gel electrodes are shown in Fig. 13. Both devices demonstrated high fidelity R-peak detection suitable for HR and HRV analysis. The primary difference in the signals is the level of baseline noises caused by the

Fig. 12. Procedure of human test design.

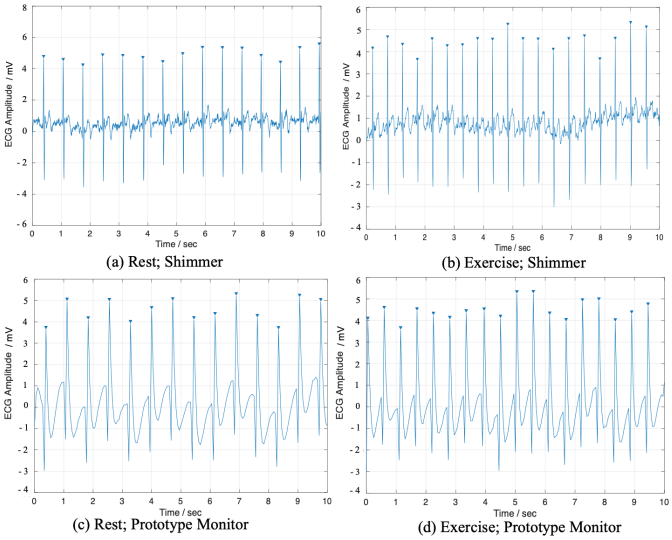

Fig. 13. R-peaks detection comparison between the commercial sensor (Shimmer 2) and our human performance monitor with AmSemi flexible Opamps version.

subject's respiration behaviors (0.2 Hz - 0.4 Hz), for which our prototype shows better mitigation effects with lower amplitude than the Shimmer device, as shown in Fig. 14.

Table III shows good agreement between the prototype monitor and the two commercial devices with respect to HR. Table IV shows the HRV parameters calculated for both the prototype monitor and the Shimmer 2 which used ionic gel based electrodes. The at-rest values show very good agreement between the prototype monitor and the Shimmer 2. The exercise HR data, show significant variations with the prototype showing more variation. This requires further work to fully understand, but is likely influenced by variations in the detected signal due to motions between the electrodes and the skin, as well as differences in HR calculation and noise cancellation algorithms used and the analog-to-digital conversion rates. The results demonstrate that the prototype with AmSemi flexible OpAmps is a viable human ECG R-peak detector, HR and HRV monitor. The Smart Watch was included in the performance tests because it is a commonly used device for monitoring HR. However, the Smart Watch was not used for HRV calculations because its function in this regard has not been certified, and it measures HR using photoplethysmography (PPG) as opposed to the continuous observation of the heart's electrical field and activity. Thus, the Smart Watch measurements were not used to calculate HRV. The Shimmer monitor, by comparison, detects the heart's electrical field as does the performance monitor reported here, and was calibrated by the manufacturer for accuracy. Thus, for HRV calculations the prototype monitor was compared to data from the Shimmer monitor.

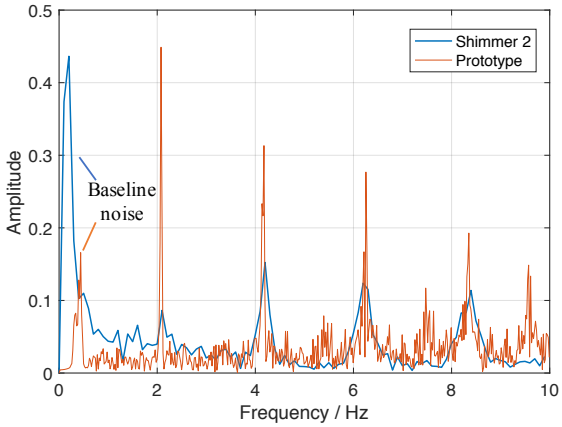

Fig. 14. Frequency analysis comparison between captured ECG signals (after exercise session) from Shimmer and our prototype respectively.

TABLE III
PERFORMANCE COMPARISON OF HEART RATE

	Test Subject		
Heart Rate (BPM)	Rest_1	Exercise	Rest_2
Smart Watch	75	117	90
Shimmer 2	78	117	91
Prototype Monitor	79	117	91

V. CONCLUSION

The interests in wearable electronics in general, and particularly for human performance and medical monitoring are rapidly expanding. This work explores the development and early application of a flexible hybrid electronics monitor for the detection of ECG signals using capacitively-coupled electrodes. These electrodes are being developed to provide a better skin-monitor interface and to eliminate the drawbacks of traditional wet-electrodes. The capacitive electrodes were fabricated on flexible polyimide substrates using an optimized electrode geometry and specialized nanolaminate dielectric fabrication method to ensure high capacitance and high signal quality while minimizing the electrode size. Custom circuitry detected R-peaks in ECG with high fidelity using only 4 op-amps. The performance of the prototype ECG monitor was verified by using simulated signals from publicly available ECG databases, and by comparing the monitor's responses with those of a smartwatch and a commercial wet-electrode based ECG sensor worn by the same human subject at the same time. The response to simulated signals was as expected, and heart rates and heart rate variabilities were comparable to the commercial devices. Thinned flexible Si-OpAmps (American Semiconductor FleX™ ASOPA4002) were shown to produce results equivalent to those produced by conventional rigid components (Texas Instrument′s LMC6442 OpAmps), indicating that such devices can provide high conformability while maintaining the high performance of Si-based electronics. These results have shown the feasibility of using capacitively-coupled ECG electrodes to produce high fidelity R-peak detection and the use of conformal thinned electronics can be equivalent to rigid, conventionally packaged devices.

ACKNOWLEDGMENT

This work was primarily funded by contract FA86501327311-7 from the NanoBio Manufacturing

TABLE IV
PERFORMANCE COMPARISON OF HEART RATE VARIANCE

Status	Exercise			Rest		
HRV[1]	SDANN[2]	RMSSD[3]	SDSD[4]	SDANN	RMSSD	SDSD
Prototype Monitor	35.9	10.6	10.7	28.7	19.6	20.9
Shimmer 2	22.5	6.6	6.6	30.6	19.8	20.3

[1] HRV: Heart Rate Variability: The HRV in the table is based on the calculation of NN intervals(ms) over 1-2 minutes
[2] SDANN: Standard deviation of the average NN intervals
[3] RMSDD: Root mean square of successive differences between adjacent NNs
[4] SDSD: Standard deviation of the successive difference between adjacent NNs

Consortium through a program sponsored by the Air Force Research Laboratory, and by Binghamton University and American Semiconductor Inc.. The U.S. Government is authorized to reproduce and distribute reprints for Governmental purposes notwithstanding any copyright notation thereon.

REFERENCES

[1] W. Gao, S. Emaminejad, H. Y. Y. Nyein, S. Challa, K. Chen, A. Peck, H. M. Fahad, H. Ota, H. Shiraki, D. Kiriya *et al.*, "Fully integrated wearable sensor arrays for multiplexed in situ perspiration analysis," *Nature*, vol. 529, no. 7587, p. 509, 2016.

[2] J. B. Wang, L. A. Cadmus-Bertram, L. Natarajan, M. M. White, H. Madanat, J. F. Nichols, G. X. Ayala, and J. P. Pierce, "Wearable sensor/device (Fitbit One) and SMS text-messaging prompts to increase physical activity in overweight and obese adults: a randomized controlled trial," *Telemedicine and e-Health*, vol. 21, no. 10, pp. 782–792, 2015.

[3] S. Preejith, R. Dhinesh, J. Joseph, and M. Sivaprakasam, "Wearable ECG platform for continuous cardiac monitoring," in *Proceedings of the 38th Annual International Conference of the IEEE Engineering in Medicine and Biology Society (EMBC)*. IEEE, 2016, pp. 623–626.

[4] E. Nemati, M. J. Deen, and T. Mondal, "A wireless wearable ECG sensor for long-term applications," *IEEE Commun. Mag.*, vol. 50, no. 1, 2012.

[5] Y. Hao and R. Foster, "Wireless body sensor networks for health-monitoring applications," *Physiological Measurement*, vol. 29, no. 11, p. R27, 2008.

[6] O. Postolache, P. S. Girao, G. Postolache, and M. Pereira, "Vital signs monitoring system based on EMFi sensors and wavelet analysis," in *Proceedings of Instrumentation and Measurement Technology Conference (IMTC)*. IEEE, 2007, pp. 1–4.

[7] S. Majumder, L. Chen, O. Marinov, C.-H. Chen, T. Mondal, and M. J. Deen, "Noncontact wearable wireless ECG systems for long-term monitoring," *IEEE Reviews in Biomedical Engineering*, vol. 11, pp. 306–321, 2018.

[8] A. Pantelopoulos and N. Bourbakis, "A survey on wearable sensor-based systems for health monitoring and prognosis," *IEEE Transactions on Systems, Man, and Cybernetics, Part C (Applications and Reviews)*, vol. 40, no. 1, pp. 1–12, 2010.

[9] B. Taji, S. Shirmohammadi, V. Groza, and I. Batkin, "Impact of skin–electrode interface on electrocardiogram measurements using conductive textile electrodes," *IEEE Transactions on Instrumentation and Measurement*, vol. 63, no. 6, pp. 1412–1422, 2014.

[10] A. Gruetzmann, S. Hansen, and J. Müller, "Novel dry electrodes for ECG monitoring," *Physiological Measurement*, vol. 28, no. 11, p. 1375, 2007.

[11] T. Torfs, C. J. Smeets, D. Geng, T. Berset, J. Van der Auwera, P. Vandervoort, and L. Grieten, "Clinical validation of a low-power and wearable ECG patch for long term full-disclosure monitoring," *Journal of Electrocardiology*, vol. 47, no. 6, pp. 881–889, 2014.

[12] B. Jeon, J. Lee, and J. Choi, "Design and implementation of a wearable ECG system," *International Journal of Smart Home*, vol. 7, no. 2, pp. 61–69, 2013.

[13] Z. Yang, Q. Zhou, L. Lei, K. Zheng, and W. Xiang, "An IoT-cloud based wearable ECG monitoring system for smart healthcare," *Journal of Medical Systems*, vol. 40, no. 12, p. 286, 2016.

[14] J. J. Oresko, Z. Jin, J. Cheng, S. Huang, Y. Sun, H. Duschl, and A. C. Cheng, "A wearable smartphone-based platform for real-time cardiovascular disease detection via electrocardiogram processing," *IEEE Transactions on Information Technology in Biomedicine*, vol. 14, no. 3, pp. 734–740, 2010.

[15] L.-D. Liao, I.-J. Wang, S.-F. Chen, J.-Y. Chang, and C.-T. Lin, "Design, fabrication and experimental validation of a novel dry-contact sensor for measuring electroencephalography signals without skin preparation," *Sensors*, vol. 11, no. 6, pp. 5819–5834, 2011.

[16] Y. M. Chi, T.-P. Jung, and G. Cauwenberghs, "Dry-contact and noncontact biopotential electrodes: Methodological review," *IEEE Reviews in Biomedical Engineering*, vol. 3, pp. 106–119, 2010.

[17] S.-J. Cho, D. Byun, T.-S. Nam, S.-Y. Choi, B.-G. Lee, M.-K. Kim, and S. Kim, "A 3D-printed sensor for monitoring biosignals in small animals," *Journal of Healthcare Engineering*, vol. 2017, 2017.

[18] M. Avenel-audran, A. Goossens, E. Zimerson, and M. Bruze, "Contact dermatitis from electrocardiograph-monitoring electrodes: role of p-tert-butylphenol-formaldehyde resin," *Contact Dermatitis*, vol. 48, no. 2, pp. 108–111, 2003.

[19] Y. Sun and X. B. Yu, "Capacitive biopotential measurement for electrophysiological signal acquisition: A review," *IEEE Sensors Journal*, vol. 16, no. 9, pp. 2832–2853, 2016.

[20] P. Griss, P. Enoksson, H. Tolvanen-Laakso, P. Meriläinen, S. Ollmar, and G. Stemme, "Spiked biopotential electrodes," in *Proceedings of IEEE 13th Annual International Conference on Micro Electro Mechanical Systems*. IEEE, 2000, pp. 323–328.

[21] Y.-H. Chen, M. O. de Beeck, L. Vanderheyden, E. Carrette, V. Mihajlović, K. Vanstreels, B. Grundlehner, S. Gadeyne, P. Boon, and C. V. Hoof, "Soft, comfortable polymer dry electrodes for high quality ECG and EEG recording," *Sensors*, vol. 14, no. 12, pp. 23 758–23 780, 2014.

[22] P. Salvo, R. Raedt, E. Carrette, D. Schaubroeck, J. Vanfleteren, and L. Cardon, "A 3D printed dry electrode for ECG/EEG recording," *Sensors and Actuators A: Physical*, vol. 174, pp. 96–102, 2012.

[23] J.-Y. Baek, J.-H. An, J.-M. Choi, K.-S. Park, and S.-H. Lee, "Flexible polymeric dry electrodes for the long-term monitoring of ECG," *Sensors and Actuators A: Physical*, vol. 143, no. 2, pp. 423–429, 2008.

[24] Y. Khan, M. Garg, Q. Gui, M. Schadt, A. Gaikwad, D. Han, N. A. Yamamoto, P. Hart, R. Welte, W. Wilson, S. Czarnecki, M. Poliks, Z. Jin, K. Ghose, F. Egitto, J. Turner, and A. C. Arias, "Flexible hybrid electronics: Direct interfacing of soft and hard electronics for wearable health monitoring," *Advanced Functional Materials*, vol. 26, no. 47, pp. 8764–8775, 2016.

[25] Y. M. Chi and G. Cauwenberghs, "Wireless non-contact EEG/ECG electrodes for body sensor networks," in *Proceedings of International Conference on Body Sensor Networks (BSN)*, 2010, pp. 297–301.

[26] Y. M. Chi, S. R. Deiss, and G. Cauwenberghs, "Non-contact low power EEG/ECG electrode for high density wearable biopotential sensor networks," in *Proceedings of Sixth International Workshop on Wearable and Implantable Body Sensor Networks (BSN)*, 2009, pp. 246–250.

[27] W. Li, O. Auciello, R. N. Premnath, and B. Kabius, "Giant dielectric constant dominated by Maxwell—Wagner relaxation in Al_2O_3/TiO_2 nanolaminates synthesized by atomic layer deposition," *Applied Physics Letters*, vol. 96, no. 162907, pp. 1–3, 2010.

[28] Z. Zhou and P. A. Warr, "A high input impedance low noise integrated front-end amplifier for neural monitoring," *IEEE Transactions on Biomedical Circuits and Systems*, vol. 10, no. 6, pp. 1079–1086, 2016.

[29] A. L. Goldberger, L. A. N. Amaral, L. Glass, J. M. Hausdorff, P. C. Ivanov, R. G. Mark, J. E. Mietus, G. B. Moody, C.-K. Peng, and H. E. Stanley, "PhysioBank, PhysioToolkit, and PhysioNet: Components of a new research resource for complex physiologic signals," *Circulation*, vol. 101, no. 23, pp. e215–e220, 2000.

[30] G. B. Moody and R. G. Mark, "The impact of the MIT-BIH arrhythmia database," *IEEE Engineering in Medicine and Biology Magazine*, vol. 20, no. 3, pp. 45–50, 2001.